International Journal of Nanomedicine

Dovepress
Taylor & Francis Group

Open Access Full Text Article

ORIGINAL RESEARCH

Camellia Sinensis Extracts Embedded in Semipermeable Nanocapsules as Active Ingredient for Dental Adhesives: Biomaterial Synthesis and Effect on the Bond to Human Dentin

Paul Richter-Mendau[1], Marioara Moldovan[2], Adrian Cernescu[3], Codruta Sarosi[2], Nicoleta Ilie[1]

[1]Department of Conservative Dentistry and Periodontology, University Hospital, Ludwig-Maximilians-University, Munich, Bavaria, Germany; [2]Institute of Chemistry Raluca Ripan, Babes-Bolyai University, Cluj-Napoca, Romania; [3]Atocube Systems AG, Haar, Bavaria, Germany

Correspondence: Nicoleta Ilie, Department of Conservative Dentistry and Periodontology, University Hospital, Ludwig-Maximilians-University, Goethestr. 70, Munich, D-80336, Germany, Email nicoleta.ilie@med.uni-muenchen.de

Purpose: This study aimed to synthesize bioactive dental adhesives using Camellia sinensis (green tea) extracts (GTE) incorporated into innovative semipermeable nanocapsules as active ingredient to stabilize the bond to human dentin.

Methods: Nanocapsules and all components of the experimental adhesives were synthesized individually, and the success of the synthesis was verified. Experimental adhesives with varying GTE levels and the current gold-standard adhesive were tested for shear bond strength (SBS) after 24-hours and 6-month aging. Bond morphology was characterized by SEM, nano-IR imaging, and fractography. The composition of the nanocapsules was evaluated using Fourier-transform infrared spectroscopy and high-performance liquid-chromatography. Phenol release was evaluated using spectrophotometry. Statistical analyses included ANOVA, Tukey HSD, Games-Howell, Kruskal–Wallis, Mann–Whitney-U, multiple *t*-tests, and Weibull analysis.

Results: The incorporation and release of polyphenols from the experimental adhesives is confirmed. A similar or slightly higher SBS was measured in the control adhesive. Aging does not have a significant impact on SBS, but the bonding reliability of the experimental adhesives remained stable over time, while the reliability of the gold-standard adhesive experienced a decline.

Conclusion: The integration of GTE-nanocapsules into an experimental adhesive proved to be a promising concept for maintaining bond strength and reliability during aging. In addition, the used combination of vibrational spectroscopy and high spatial resolution of atomic force microscopy proved to be helpful in closing a nano-analytical diagnostic gap in the molecular spectroscopy of dental nanomaterials.

Keywords: dental adhesives, nanocapsules, green tea extract, polyphenols, bond strength, reliability

Introduction

The exponential growth observed in the development of nanoparticles over the last two decades has also resulted in new approaches to tackle a range of issues in medicine and dentistry. According to the International Union of Pure and Applied Chemistry (IUPAC), a nanocapsule is defined as a hollow nanoparticle composed of a solid shell surrounding a core-forming space available to entrap substances.[1] A wide range of biodegradable materials can be used to construct this solid shell, including lipids (such as cholesterol, phosphatidylcholine, and phosphatidylserine), metals (such as silver, iron oxide, zinc oxide, aluminum oxide, copper oxide, and gold), and natural and synthetic polymers (eg, poly[lactic-co-glycolic] acid (PLGA) and polylactic acid (PLA)).[2] Due to these characteristics, nanocapsules offer a wide range of benefits in the medical field. So far, they have been successfully employed to improve food products, such as in supporting food preservation[3] or improving the stability of degradable compounds,[4] and to develop self-healing materials[5] and drug delivery. The latter is based on their capacity to encapsulate poorly soluble drugs,[6] improve protection against intracellular and extracellular degradation in

Received: 2 April 2025
Accepted: 4 July 2025
Published: 25 July 2025

comparison to unencapsulated pharmaceuticals,[7] and alter blood circulation and tissue distribution of the active agents.[8] In addition, they have proven successful in several medical fields, including oncology,[9] and in immunology.[10]

As the idea of nanocapsules was proposed by Richard P. Feynman more than 60 years ago,[11] the development of new methodologies aimed at enhancing the durability of the capsules and their capacity for targeted drug release continues. In this line of events, Hitchcock et al proposed a method for integrating oil-based agents into metal shells, thereby reducing the leakage of the filled substance and controlling its release via ultrasound.[12] Dentistry has also implemented nanotechnology and uses the new possibilities of targeted drug release from nanocapsules. As such, the use of ionic liquids (ILs), organic salts with a low melting point and antibacterial properties,[13] has become established in dentistry as an alternative to conventional pharmaceutical salts. This is due to the tendency of pharmaceutical salts to undergo crystal polymorphism in pharmaceutical compounds, a process that ILs do not undergo.[14] The design of dental resin infiltrants with drug delivery systems incorporating ILs represents a promising approach for enhancing materials used in restorative and micro-invasive dental treatments.[15] Another benefit of nanocapsules used in modern dental materials is their ability to provide graded release through diffusion or erosion.[16] Priyadarshini et al applied this effect to deliver Chlorhexidine (CHX), a proven dental antibacterial agent,[17] in the form of polymer-coated nanoscales capsules to demineralized dentin substrates through dentin tubules to ensure a more extended release of the drug and a higher persistence.[18]

One of the critical effects of CHX is the inhibition of a variety of matrix metalloproteinases (MMPs), which contribute, together with cysteine cathepsin, to collagen enzymolysis.[19] Collagen enzymolysis is one of the primary factors compromising the stability of the bond, along with the degradation of the hybrid layer at the adhesive-dentin interface caused by adhesive hydrolysis and the formation of secondary caries.[19] MMPs are a group of calcium- and zinc-dependent, host-derived enzymes,[20] which are trapped between the collagen fibrils during dentinogenesis.[21] A large number of MMPs can be found all over the human body. However, in the dental tissue, the gelatinase MMP-2 and MMP-9,[22] stromelysin MMP-3,[23] enamylesin MMP-20,[24] cysteine cathepsin,[25] MMP-14 and the collagenase MMP-8[26] are particularly abundant. Research shows these MMPs are mainly released by polymorphonuclear leukocytes, macrophages,[27] and dentin-forming odontoblasts.[26] In the dentinal environment, these enzymes play a major role in the development of intra- and intertubular dentin[28] and dentin maturation[29] but also in the development of dentin caries[30] and the breakdown of collagen, mainly type I collagen.[31] MMPs are able to deteriorate the dentin organic matrix after demineralization, which leads to hydrolysis and, therefore, a weakening of the dentin bonding strength.[32] Studies show that an acidic environment, eg, provided by a 37 wt.% phosphoric acid gel in an etch and rinse approach, is able to activate MMP secretion but will denature the enzymes due to its relatively strong pH.[33] Due to their acidic monomer groups, modern self-etch adhesives will also activate these MMPs. Yet, they cannot denature these activated enzymes due to their pH being around 1 or 2 and, therefore, much milder.[34] Due to this contrast in their ability to denature enzymes, etch-and-rinse and self-etch systems influence the degree of MMP activity remaining in the hybrid layer differently resulting in the usage of a self-etch approach to conduct this study as it allows an isolated evaluation of the effects of GTE as an MMP inhibitor without interference from other factors such as phosphoric acid. However, it is not only the activity of the host-derived proteinases that has a negative impact on the bond strength; insufficient infiltration after etching also appears to be a cause of denaturation and, thus, loss of bonding.[35] Counteracting this impact on bond strength has been a core question in dentistry for some time, as too strong self-etch adhesives can dissolve calcium phosphate from the hydroxyapatite of the tooth structure in an etch-and-rinse-like manner, leaving the exposed calcium to weaken the interface integrity due to a lack of rinsing. Mild self-etch adhesives have proven effective in reducing the imbalance of deep demineralization and infiltration by creating a more shallow demineralized area.[36] In the matter of MMPs, it seems impossible to entirely banish them from the areas to be bonded, leaving researchers with only one option: alleviating their effects.

This context provides one of the baselines for this study's hypothesis, as encapsulated polyphenols – known for their MMP-inhibitory and collagen-stabilizing properties – may counteract enzymatic degradation of the adhesive morphology.

Compounds found in *Camellia sinensis*, commonly known as tea, have caught researchers' interest in this particular matter. Tea, which is shown to be, aside from water, the second most consumed beverage on the planet,[37] has been known for its positive effects on the human body for centuries.[38] Especially the manufacturing of green tea aims at the preservation of catechins, a subgroup of polyphenols and the predominant group of substances in this beverage, due to its way of plucking, steaming, rolling, and high-temperature air drying.[37] It is suggested that polyphenols are likely to fulfill specific roles in the

medical treatment of diseased under three distinctive general characteristics: Their ability to form complexes with metal ions, exhibit antioxidant and free radical scavenging activities, and bind with various other molecules, including macromolecules like proteins and polysaccharides.[39] Additionally, they have been proven to inhibit several pathogenic factors of *Streptococcus mutans* at both the transcriptional and enzymatic level responsible for caries.[40] This makes them an essential compound in general medicine and dentistry and conducts the reason why these compounds were used in this study instead of other MMP inhibitors. Additionally, the polyphenols found in *Camellia sinensis* also exhibit a collagen crosslinking effect, further enhancing their value in application.[41]

Various research has been conducted over recent years to identify the most effective method for applying polyphenols to dentin. This has resulted in the development of two primary approaches. The first approach combines the active agent with an aqueous[42] or ethanol[43] solution and applies it as an additional step during the bonding protocol. This approach has shown positive effects on the retention of the SBS over time[44] but is more time-consuming and, therefore, less user-friendly. An alternative approach is adding the active agent to the bonding agents, eliminating the extra step in pretreatment.[45,46] Although this approach appears favorable regarding user-friendliness and time-saving, incorporating additional components into an existing system may impact its properties, such as bond strength.[47]

The present study aimed to investigate the potential of combining the effects of polyphenols with new drug delivery and release opportunities by incorporating them into permeable nanocapsules as part of an experimental adhesive. Therefore, experimental adhesives with different capsule concentrations were synthesized and tested for their ability to prevent deterioration in the bonding of composite materials to dentin due to aging and hydrolysis. The hypotheses tested state that the addition of encapsulated polyphenols to experimental adhesives hindered hydrolytic degradation by up to 6 months compared to the current gold standard adhesive, with the effect depending on the concentration of the active ingredient.

Materials and Methods

Three experimental mild two-step self-etch adhesives were synthesized and compared to a gold-standard adhesive that served as a positive control. The bond strength was determined using a standardized shear-bond strength test (SBS) and followed by fractographic analysis. In addition, representative specimens were also analyzed using scanning electron microscopy (SEM) and nano-IR imaging. The experimental adhesives are in the following referred to as A1-3 (Table 1), with A1 defining the experimental adhesive containing no green tea extract (GTE) infused nanocapsules. A1 served as the basis for the production of the experimental adhesives A2 and A3, with 1 wt% of GTE-nanocapsules being infused into adhesive A2 and 2 wt% into adhesive A3. The adhesive, Clearfil SE Bond (Kuraray Noritake Dental Inc. Kurashiki, Japan), will be referred to as CSE and served as the gold-standard control group. Clearfil SE Primer (Kuraray Noritake Dental Inc. Kurashiki, Japan) was used as primer for all adhesives to allow for direct comparison. Evaluation of the bond strength and morphology of the adhesive-dentin interface was conducted in an initial state (24h post-polymerization and

Table 1 Chemical Composition of the Analyzed Composite and Adhesives

Name	Components	LOT No
AF	Ormocer, 84 wt%, Ba-Al-Si-glass	2111693
CSE Primer	10-MDP, HEMA, DM, Initiators	5P0431
CSE Bond	10-MDP, bis-GMA, Hema, DM, Initiators Bis-GMA, HEMA, TEGDMA, polyacrylic Acid, Cq, Ethyl 4-dimethylaminobenzoate	6P0885
A1	Bis-GMA, HEMA, TEGDMA, polyacrylic Acid, Cq, Ethyl 4-dimethylaminobenzoate	
A2	Bis-GMA, HEMA, TEGDMA, polyacrylic Acid, Cq, Ethyl 4-dimethylaminobenzoate, 1wt% GTE-nano-capsules	
A3	Bis-GMA, HEMA, TEGDMA, polyacrylic Acid, Cq, Ethyl 4-dimethylaminobenzoate, 2 wt% GTE-nano-capsules	

Abbreviations: AF, Admira Fusion x-tra; Ba-Al-Si-glass, barium-aluminum-silicate-glass; CSE, Clearfil SE; 10-MDP, 10-methacryloyloxydecyl-dihydrogenphosphate; HEMA, 2-hydroxyethyldimethylacrylate; DM, dimethylacrylate; bis-GMA, bisphenol-A-diglycidyl-methacrylate; TEGDMA, triethylene-glycol-dimethacrylate; Cq, camphorquinone; ormocer, organically modified ceramic; GTE, green tea extract.

https://doi.org/10.2147/IJN.S525646

immersion in distilled water at 37°C in the dark) and after an aging process (6 months under identical conditions and replacement of the immersion medium each week).

Synthesis of Green Tea Extract (GTE) – Nanocapsules

The method used for preparing nanocapsules in this study was the interfacial deposition technique, achieved by mixing an organic and aqueous phase. The organic phase contains acetonitrile (Sigma-Aldrich Inc.), Miglyol® 810 N (IOI Oleo GmbH, Witten, Germany), 1% hydroxyapatite crystallized at 1100°C for 2 hours, and green tea extract. The GTE was manufactured by pulverizing 4 g of green tea leaves (Twinings of London, AB Food & Beverages Australia Pty. Ltd., Rowville, Victoria, Australia) which were then dissolved in 20 mL of 96% ethanol (Maraton 92 Impex SRL, Bucharest, Romania). The extraction of the active components from green tea was conducted for 30 min. at room temperature (23°C). After decanting the resulting extract was transferred to an Elmasonic P 70 H ultrasonic bath (Elma Schmidbauer GmbH, Singen, Germany) set to 30°C for two 15-minute cycles followed by another 15-minute cycle at 60°C. To conclude the process, the solution underwent centrifugation (Sigma 1–6, Sigma Laborzentrifugen GmbH, Osterode am Harz, Germany) at 3000 rpm for 10 min. The liquid phase was then isolated and used to prepare dental adhesives. The aqueous solution consisted of Poloxamer 407 (Sigma-Aldrich Inc.), green tea extract, and acetonitrile (Sigma-Aldrich Chemie GmbH, Taufkirchen, Germany). The organic solution was added to the aqueous phase and emulsified using an Ultra-Turrax® T8 rotor-stator device for 10 minutes. Distilled water, equivalent to five times the volume of the emulsion, was added to the emulsion under mild stirring. The mixture was stirred for 15 minutes at 9.000 rpm. By evaporation under reduced pressure, the organic solvent and part of the water were removed to obtain a refined suspension. The final diameter of the nanocapsules ranged between 200 and 350 nm. This method combines interfacial phenomena during solvent diffusion and polymer precipitation, providing a regulated method to encapsulate active ingredients and form nanocapsules. Figure 1 shows an illustration of the method described above.

Synthesis of Experimental Adhesives

The organic matrix consists of 97% by weight of a monomer mixture combined with various additives. Bis-GMA oligomers (synthesized in the UBB) were incorporated along with diluting monomers such as TEGDMA (triethylene glycol dimethacrylate) and HEMA (hydroxyethyldimethylacrylate). To create an acidic pH, polyacrylic acid was included and dissolved entirely in HEMA. The photoinitiator system incorporates the polymerization accelerator ethyl-4-dimethylaminobenzoate at 1 wt.% as well as the photosensitizer camphorquinone (CQ) at 0.5 wt.% of the monomer mixture. As an UV stabilizer BHT (2,6-di-tert-butyl-4-methylphenol) was included. Additives, such as the UV stabilizer,

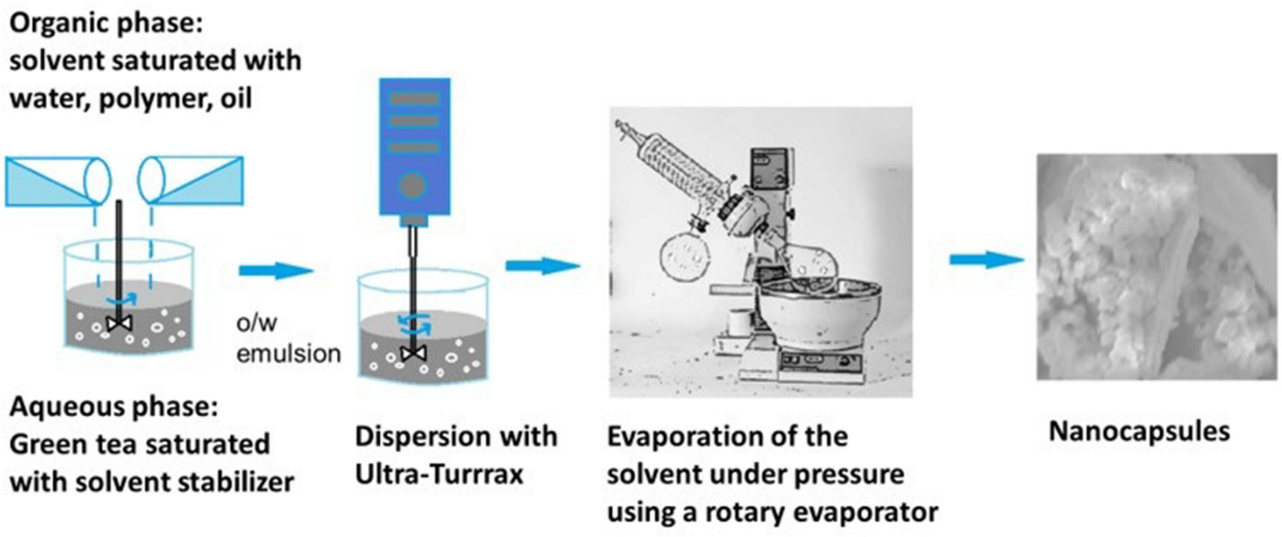

Figure 1 Preparation of nanocapsules by the interfacial deposition technique.

antioxidant, photosensitizer, and the polymerization accelerator, inhibitor and initiator comprise 3% of the total weight. To the prepared liquid, 1 wt.% and 2 wt.% nanocapsules containing green tea extract were added and mixed until a homogeneous composition was achieved. The resulting adhesive with green tea nanocapsules has a pH of 4.

Fourier-Transformed Infrared Spectroscopy (FTIR)

Further investigation of the prepared adhesives and nanocapsules occurred by Fourier-transformed infrared spectroscopy (FTIR). Compact discs with dimensions of 1×1 mm of the polymerized adhesives with nanocapsule as well as the nanocapsules were used for scanning. Therefore, an FTIR 610 spectrometer (Jasco Corporation, Tokyo, Japan) fitted with an ATR attachment (attenuated total reflectance) and featuring a horizontal ZnSe crystal (Jasco PRO400S) in the 4000–500 cm^{-1} wave number range was employed. Spectral resolution was set to 4 cm^{-1} while completing 100 scans for each measurement at room temperature. The interpretation of the spectra was guided by B.C: Smith's *Infrared Spectral Interpretation: A Systematical Approach*, which served as a reference for identifying important functional groups.[48]

High-Performance Liquid Chromatography Analysis

Organic acids, carbohydrates, and Individual phenolic compounds (phenolic acids and flavonoids) were analyzed using a high-performance liquid chromatography (HPLC). Therefore, a Jasco Chromatograph (Jasco Corporation, Tokyo, Japan) was fitted with an injection valve attached to a 20 µL sample loop (Rheodyne) and a UV/Vis detector. To operate the HPLC system and collect and process the chromatographic data, the ChromPass Software was employed. The HPLC analysis of individual phenolic compounds occurred by using the HPLC gradient analysis method defined by Filip et al.[49] Phenolic acids and flavonoids were separated at 22°C column temperature with UV detection set at 270 nm on the Lichrosorb RP-C18 column (25 × 0.46 cm). A combination of 0.1% formic acid solution (Millipore ultrapure water) and methanol (A, HPLC grade) was used for the mobile phase. The following method was conducted to implement a gradient at a flow rate of 1 mL/min: linear gradient 10–25% A, 0–10min; linear gradient 25–30% A, 10–25 min; linear gradient 35–50% A, 25–50 min; isocratic 50% A, 50–70 min.

Spectrophotometrical Analysis (Folin-Ciocalteu Method)

To determine the total polyphenolic compounds (TPC) spectrophotometrically a Folin-Ciocalteu (FC) reagent was used.[50,51] Therefore, 0.4 mL of methanolic sample extract and 2 mL of FC reagent (diluted 1:1) were shaken for 3 min followed by including 1.6 mL of sodium carbonate solution (7.5%). The mixture was then raised to 10 mL using water. After incubation for 10 minutes at 50°C, the solutions were allowed to cool, and the absorbance was recorded at 760 nm in contrast to a reagent blank (1.6 mL sodium carbonate solution + 2 mL FC reagent + 0.4 mL water). The samples' absorbance of gallic acid (GAE) standards were recorded. The TPC of each extract was quantified as mg gallic acid equivalent per 100 g dry weight (mg GAE/100 g).

Specimen Preparation for Shear Bond Strength (SBS) Testing

A total of 40 human third molars, extracted no longer than three months and continuously stored in 0.2% sodium azide water (Merck KGaA, Darmstadt, Germany) at room temperature, were used for specimen preparation (ethical approval KB 20/032). The teeth were cut horizontally at the enamel-cementum junction and above the pulp chamber, ensuring the cut was made as centrally as possible between the pulp chamber and the enamel-dentin junction to separate the roots from the crown and expose mid-coronal dentin. A third, now vertically performed cut was made, dividing each tooth into four specimens. All cutting was performed using a water-cooled, low-speed diamond saw (IsoMet, Buehler, Lake Bluff, IL, USA). Immediately after cutting, the segments were embedded in a methyl methacrylate polymer (Technovit 4004, Kulzer, Hanau, Germany) using a stainless-steel cylinder with a 16 mm diameter to allow the dentin surface to protuberate. The prepared specimens were then randomly divided into eight groups (n=20) based on the adhesive system used (CSE, A1, A2, A3) and the storage duration prior to testing (24h or 6 months). Specifically, groups 1 to 4 included CSE, A1, A2, and A3 tested after 24 hours, respectively, while groups 5 to 8 consisted of the same adhesives tested after 6 months. Prior to bonding, the tooth surface was ground under running water with 600-grit silicon carbide grinding paper (Leco, St. Joseph, MI, USA) for 20 seconds to create a clinically similar smear layer. CSE Primer was applied as recommended by the manufacturer (applied for 20 seconds and gently dried with air) using single-use microbrushes.

Following priming, the adhesives were applied using the same technique based on the guidelines for CSE. The adhesive was added using a fresh microbrush and gently dried by airflow until no movement was visible. Finally, a 10-second light curing phase was conducted using a violet-blue LED LCU (Bluephase® Style Ivoclar Vivadent, Schaan, Liechtenstein) with a light-emitting window of 10 mm² and a mean irradiance of 1366.6 ± 3.8 mW/cm². A spectrophotometer (Managing Accurate Resin Curing, Bluelight Analytics Inc., Halifax, Canada) was used to determine irradiance, radiant exposure, and spectral distribution (n=3). This device was used for all light-curing steps conducted in this study. Following priming and bonding, a cylindrical resin-based composite (RBC) structure, having an approximate height of 3 mm and a circular area of approximately 4.52 mm² (the exact area was determined for each specimen in microscopic evaluation), was attached to the conditioned area. Therefore, all specimens were fixed into a matrix holder (Ultradent Products, South Jordan, UT, USA). The RBC (AF, Admira Fusion x-tra VOCO GmbH, Cuxhaven, Germany) was then applied using a cylindrical split mold (Ultradent Products, South Jordan, UT, USA).

Shear Bond Strength Testing

A universal testing machine (Z2.5, Zwick/Roell, Ulm, Germany) was loaded with the specimen and used for conducting SBS tests at a crosshead speed of 0.5 mm/min until failure. The maximum load upon failure was measured and divided by the bonding area measured via light microscopy to calculate the SBS. ISO-29022[52] was used with a straight edge rather than a notched edge chisel to carry out these tests.

Fractographic Analysis

To perform fractographic analysis all fractured specimens were examined on both surfaces (dentin and composite) microscopically (Stemi 508, Carl Zeiss Microscopy GmbH, Göttingen, Germany), photographed using a camera setup (Axicom color 305, Carl Zeiss Microscopy GmbH, Göttingen, Germany) and interpreted using the AxioVision software (Carl Zeiss Microscopy GmbH, Göttingen, Germany). Fracture modes were classified as adhesive failure (fracture line only in the adhesive layer) and cohesive failure (fracture line in the adhesive layer and dentin or composite). The adhesive failure was additionally divided into an adhesive failure of the adhesive layer, meaning it detached entirely from one of the substrates (dentin or composite), and a mixed failure, in which the adhesive layer remained partially bonded to the composite and partially to the dentin.

SEM Evaluation

Eight additional human third molars were randomly selected according to the abovementioned criteria and split into two groups (n=4) according to their designated aging condition of either 24h or 6 months. To conduct a sandwich technique, a tooth was cut horizontally at the dentin-cement junction and above the pulp chamber, followed by the aforementioned grinding, priming, and adhesive application. For each of the eight dentin specimens, sourced from the four teeth of one condition, one of the four adhesives was applied to the surface oriented coronally, and a different adhesive to the surface oriented apically. This method ensured that each adhesive was used twice, once on a coronal and once on an apical surface, across all eight specimens. The RBC was placed between the two tooth halves and evenly distributed by applying pressure. Polymerization occurred from each side of the tooth for 40 seconds to ensure the RBC was entirely cured. After preparation, the specimens were stored according to their designated aging condition for 24 hours or 6 months in distilled water and a dark environment at 37°C. After aging was completed, the tooth was cut vertically and wet-finished using an automatic polishing machine (EXAKT Advance Technologies GmbH, Norderstedt, Germany) with different grain-sized silicon carbide abrasive papers (P1200, P2500, P4000), followed by polishing with diamond sprays (6 µm, 3 µm, 1 µm; DP-Spray, Struers GmbH, Puch, Austria) and a polishing cloth (DP-Pan, 200 mm, Struers GmbH). After rinsing and air drying, the specimens underwent a 30-second demineralization process in a 6 mol/L hydrochloric acid solution (Sigma-Aldrich Co., St. Louis, MO, USA), followed by 10 minutes of deproteinization in a 12% sodium hydroxide solution (Sigma-Aldrich). Pure ethanol concentrations were used to ensure dehydration in an ascending order, starting at 25% ethanol in water for 20 minutes, followed by 50% ethanol (20 minutes), 75% ethanol (30 minutes), 95% ethanol (30 minutes), and ending at ≥99.8% ethanol for 60 minutes. All specimens were sputtered with gold prior to

observation of the adhesive thickness using an electron microscope (Zeiss Supra 55 VP, Carl Zeiss AG, Oberkochen, Germany) at a magnification rate of 1000x at 10 kV.

In addition to the SEM evaluation of the bonding morphology, further SEM evaluation of the adhesives was performed to verify uniform distribution of the nanocapsules.

Nano-IR sSNOM Imaging

Sub-diffraction nano-IR imaging of tooth samples was performed using a scattering scanning near-field optical microscope (IR-neaSCOPE+s, attocube systems AG, Germany). Deep Class I cavities were prepared in four additional teeth and restored with the adhesives described above. After storage in distilled water at 37°C for 24 hours, the tooth was cut in half, and the exposed surface was ground and polished similarly to the procedure described above. The sample surface was scanned with a 20 nm radius AFM tip (Pt/Ir-coated, ARROW-NCPt from NanoAndMore GmbH, Germany), providing topographic information. The tip was illuminated at a specific wavenumber using a quantum cascade laser (MIRCAT, Daylight Solutions), which simultaneously acted as a light-concentrating antenna, allowing nanofocused optical probing of the sample. The AFM operated in tapping mode (approx. 60 nm amplitude), modulating the near-field interaction between the tip and sample. An asymmetric Michelson interferometer, paired with lock-in detection at a higher harmonic of the tapping frequency (~250 kHz), enabled background-free nano-IR absorption and reflectivity mapping of the sample area, achieving spatial resolution dictated by the AFM tip, independent of the laser wavelength.

Statistical Analysis

Data analysis took place using SPSS (IBM SPSS Statistics, Version 29, International Business Machines Corporation, NY, USA). It focused on the effect of bonding agent and storage time on shear bond strength. Shapiro–Wilk tests were conducted to verify normal distribution, followed by Levene's test to determine equality of variances. In the case of a normal distribution, a one-way ANOVA with Tukey HSD and Games-Howell posthoc tests were done to determine whether the means of a dependent variable differs across more than two independent samples. In the case of a not-normal distribution, a Kruskal–Wallis-Test was performed. Using a series of Student's t-tests, the influence of aging on each adhesive was identified. A two-way ANOVA was performed to gain information about the influence of each variable (concentration of GTE and aging). Results from each test were considered significant for $p<0.05$ (95% confidence level). Weibull analyses were conducted for each adhesive and aging condition to determine the bond strength's reliability. A series of tests containing the Shapiro–Wilk test, Levene's test, Mann–Whitney-U- and Kruskal–Wallis-Test was later conducted for datasets excluding the specimens with cohesive failures determined in the fractographic analysis.

Ethics Statement

The research study was performed in accordance with the principles stated in the Declaration of Helsinki. The protocol of the study has been approved by the ethics committee of the Ludwig-Maximilians University Munich (LMU), Germany, and received the Project No: 22–0472 KB; The chairman of the Ethics Committee was Prof. Dr. R. M. Huber; The LMU's ethics committee confirms that there is no obligation to advise for the above research project by the ethics committee, and the work with anonymized extracted teeth was allowed. At the request of the treating dentists, the patients gave their verbal consent for the anonymous collection and use of their extracted teeth for research purposes.

Results

Fourier-Transformed Infrared Spectroscopy (FTIR)

Figure 2 shows the FTIR spectra for the prepared nanocapsules individually (NC) and embedded into the adhesive (Adhesive NC). The interaction of their chemical bonds with the infrared beam causes specific vibrations, such as stretching and bending, which result in characteristic absorption bands described in Table 2. The peak at 1717 cm^{-1} can be assigned to the polyphenols present in the capsules. However, since it represents the saturated C=O stretching vibration, this assignment is not exclusively applicable to polyphenols, as it also belongs to the photoinitiator or the monomers.

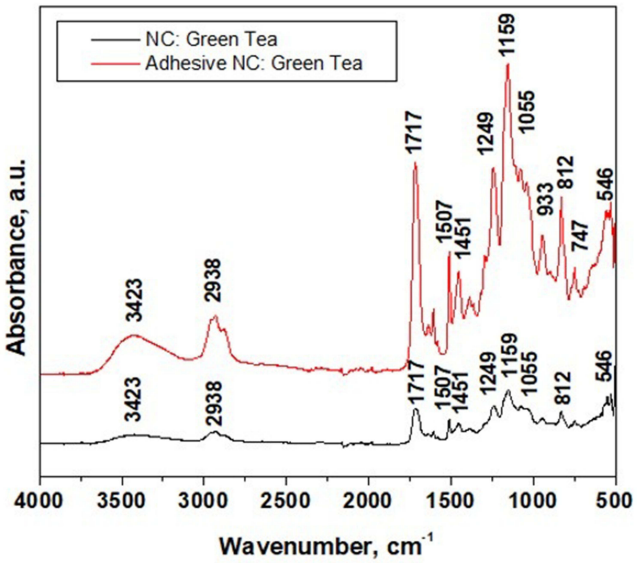

Figure 2 FTIR spectra of the nanocapsules (NC) evaluated individually and embedded in the synthesized adhesive.

High-Performance Liquid Chromatography Analysis (HPLC)

The results of the HPLC analysis are shown in Figure 3, summarizing the chromatograms of the used standards of flavonoids and phenolic acids in comparison to the values measured in the green tea extract before incorporation into the nanocapsules and the nanocapsules infused with the green tea extract. The mass of catechins identified by HPLC within the green tea extract and the nanocapsule with green tea extract is displayed in Table 3. Catechin is shown to be the dominant polyphenol both in the green tea extract and the capsule infused with it.

Spectrophotometrically Analysis (Folin-Ciocalteu Method)

The total polyphenolic content measured spectrophotometrically was quantified as mg gallic acid equivalent per 100 g dry weight (mg GAE/100 g) and gave a content of 45.711 mg/g in the nanocapsules with green tea extract and 3.35 mg/g in the experimental adhesive with 2% nanocapsules with green tea extract.

Table 2 Absorption Bands Assignment

Wavenumber (cm^{-1})	Assignment	Compound
3423	O-H stretching	-OH from in water and aromatic phenolic compound
2938, 2825	C–H stretch	$-CH_2$/$-CH_3$ groups
1717	Saturated C=O stretch	Polyphenols
1507	C—H bending	Epoxy
1451	CH_3-O	CH_3 umbrella mode
1249	C–O stretch	Phenols
1159	C-O-C asymmetric	Ethers
1055	C-O stretch	Alcohols, aromatic phenols
933	O-H out of plane	Carboxylic acids
812	C-H bending	Benzene ring
747	C-H bend out of plan	Alkene
546	PO_4^{3-} bend	Hydroxyapatite

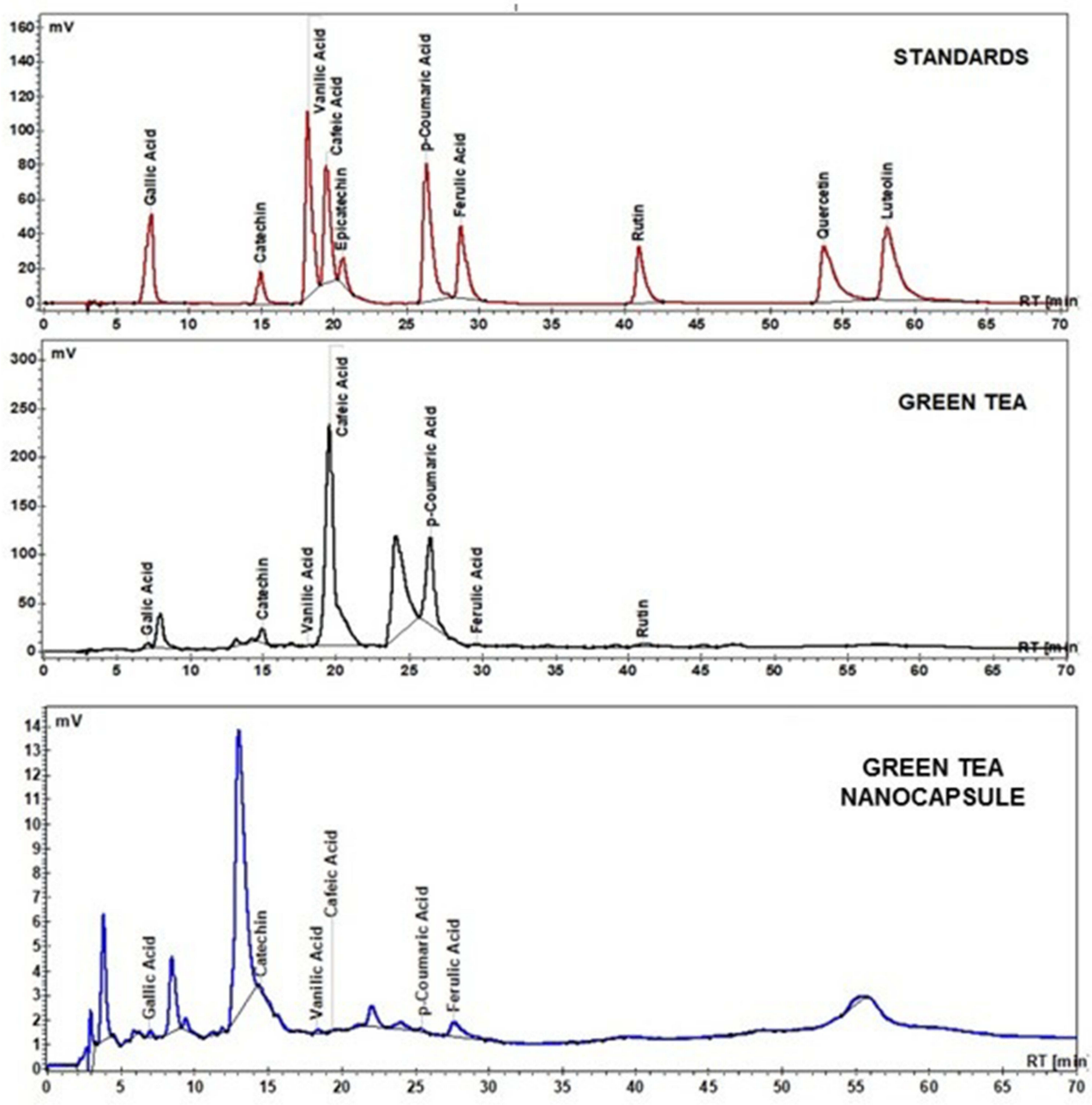

Figure 3 HPLC chromatograms of standards of flavonoids and phenolic acids, green tea extract, and the nanocapsules infused with the green tea extract.

Shear Bond Strength

In Table 4, the SBS and Weibull statistics are summarized. The Shapiro–Wilk test revealed a normal distribution for the control group (CSE) and the experimental adhesive A2 across both aging conditions, while A1 and A3 demonstrated non-normal distributions. Consequently, both a one-way ANOVA and a Kruskal–Wallis-Test were applied. Levene's test confirmed the homogeneity of variances across the aging conditions. For the 24-hour immersion, the Tukey HSD indicated significant differences between CSE and A1 ($p = 0.010$) and between CSE and A3 ($p = 0.006$). No significant differences were observed among the experimental adhesives. After six months, CSE exhibited significantly higher values in comparison to A3 ($p = 0.002$) and A2 ($p = 0.025$), but not A1 ($p = 0.116$), while A1, A 2, and A3 remained statistically indistinct from one another. The Kruskal–Wallis test corroborated a significant variation across adhesives for the 24-hour ($p = 0.002$) and six-month ($p = 0.006$) data sets. Student's t-tests revealed no statistically significant effect of

https://doi.org/10.2147/IJN.S525646

Table 3 Mass of Compounds Identified by HPLC

Phenolic Compounds	Green Tea Extract (GTE) [mg/g]	Nanocapsule with GTE [µg/g]
Gallic Acid	1.408 ± 0.11	90.7 ± 0.77
Catechin	4.586 ± 0.38	948.9 ± 8.91
Vanillic Acid	0.036 ± 0.005	100.5 ± 11.03
Caffeic Acid	36.665 ± 3.94	26.8 ± 3.04
p-Coumaric acid	8.438 ± 0.93	96.7 ± 0.89
Ferulic Acid	0.280 ± 0.08	1509.1 ± 98.2
Rutin	1.144 ± 0.11	90.7 ± 7.62

Table 4 SBS in MPa (Mean ± Standard Deviation), Along with the 95% Confidence Interval for the Weibull Modulus, Provided in Parentheses. The Different Superscript Numbers ($^{1,\ 2}$) Indicate a Statistically Significant Difference in SBS Between Materials Under Similar Aging Conditions

Adhesive	24h			6 months		
	SBS	m	R^2	SBS	m	R^2
CSE	12.2^{1}	2.8	0.97	11.3^{1}	2.1	0.90
	(5.0)	(2.5; 3.1)		(4.5)	(1.7; 2.4)	
A1	7.1^{2}	2.0	0.95	$7.9^{1,2}$	1.5	0.85
	(4.5)	(1.7; 2.2)		(5.4)	(1.2; 1.8)	
A2	$8.2^{1,2}$	1.4	0.96	6.9^{2}	1.4	0.92
	(5.1)	(1.3; 1.6)		(4.1)	(1.2; 1.6)	
A3	6.9^{2}	1.5	0.97	5.7^{2}	1.2	0.97
	(5.3)	(1.3; 1.6)		(4.9)	(1.1; 1.3)	

aging on any adhesive (eg, CSE p = 0.273). A two-way ANOVA further confirmed the non-significant influence of aging (p = 0.412; ηp^2 = 0.004) but identified a significant effect of adhesive type on SBS values (p < 0.001; ηp^2 = 0.158). Regarding the Weibull modulus, significant differences were established when the 95% confidence intervals did not intersect. For the 24-hour immersion period, the Weibull modulus decreased significantly in the sequence CSE > A1 > (A2, A3). After six months, significant differences were observed only between CSE and both A2 and A3. The aging process had a negative impact on the Weibull modulus in CSE, whereas it remained stable in the experimental adhesives.

Since cohesive failure does not reflect bond strength, a statistical analysis was conducted, including only adhesive fractures (Table 5). Data of adhesive fractured specimens was normally distributed in all adhesives with 24 hours of storage (Shapiro–Wilk test: CSE: p=0.807; A1: p=0.754; A2: p=0.251; A3: p=0.498), while only in two adhesives (CSE: p=0.935 and A2: p=0.052) at 6-month immersion. (A1: p=0.024 and A3: p=0.022).

Given the differing sample sizes in each group, due to the elimination of the cohesive fractured specimens, Kruskal–Wallis and Mann–Whitney-*U* tests were employed. Within both aging conditions, only CSE-A3 (p=0.040) at 24h immersion differed significantly from each other (Table 6), while aging showed no effect (Mann–Whitney-*U* test:

Table 5 SBS in MPa (Mean ± Standard Deviation), Along with the 95% Confidence Interval for the Weibull Modulus, Which is Provided in Parentheses for Exclusive Adhesive Fractures. The Different Superscript Numbers ([1, 2]) Indicate a Statistically Significant Difference in the Data Set of SBS Between Materials Under Similar Aging Conditions

Adhesive	24h				6 months			
	n	SBS	m	R^2	n	SBS	m	R^2
CSE	9	8.2[1]	3.6	0.98	12	9.0[1]	1.9	0.87
		(2.6)	(3.1; 4.1)			(3.7)	(1.4; 2.4)	
A1	14	5.4[1,2]	2.2	0.96	17	6.2[1]	1.6	0.81
		(2.5)	(2.0; 2.5)			(3.9)	(1.2; 2.0)	
A2	13	5.9[1,2]	1.4	0.95	18	6.8[1]	1.3	0.91
		(3.8)	(1.2; 1.6)			(4.3)	(1.1; 1.5)	
A3	15	4.6[2]	1.8	0.95	18	4.7[1]	1.3	0.97
		(2.7)	(1.5; 2.0)			(3.8)	(1.2; 1.4)	

Table 6 Statistical Significance Tested with a Kruskal–Wallis-Test Comparing the Ranks of Each Adhesive in Both Aging Conditions with Adhesive Failure

	24h	6 months
CSE - A1	p = 0.248	p = 0.781
CSE - A2	p = 0.507	p = 1.000
CSE - A3	p = 0.040	p = 0.066
A1 - A2	p = 1.000	p = 1.000
A1 - A3	p = 1.000	p = 1.000
A2 - A3	p = 1.000	p = 1.000

CSE: U = 46,000, Z = −0.569, p = 0.602; A1: U = 107,000, Z = −0.476, p = 0.645; A2: U = 102,000, Z = −0.601, p = 0.560; A3: U = 121,000, Z = −0.506, p = 0.630) using the exact sampling distribution of U.[53]

With 24h immersion, the reliability (m) decreases in sequence CSE > A1 > (A2, A3), while after aging, it becomes statistically the same for all adhesives. Aging decreased reliability in CSE and A3 and maintained it in A1 and A2.

Fractographic Analysis

The most prevalent failure mode was the adhesive failure, observed in 116 out of 160 specimens, representing a total of 72.5%. When the 24-hour aging condition is considered in isolation, adhesive remains the predominant fracture mode (63.8%), although it is lower than the total. The CSE control group, at 55%, is the only group in which cohesive failures occurred as the primary fracture mode. Adhesive failures increased from 63.8% after 24 hours to 81.25% with aging. In adhesive fractures in which the adhesive partially adhered to the dentin and partially to the composite, which was defined as adhesive mixed failure, the adhesive predominantly adhered to the composite for the experimental adhesives and to the dentin for CSE. The exact distribution of the failure modes can be found in Figure 4.

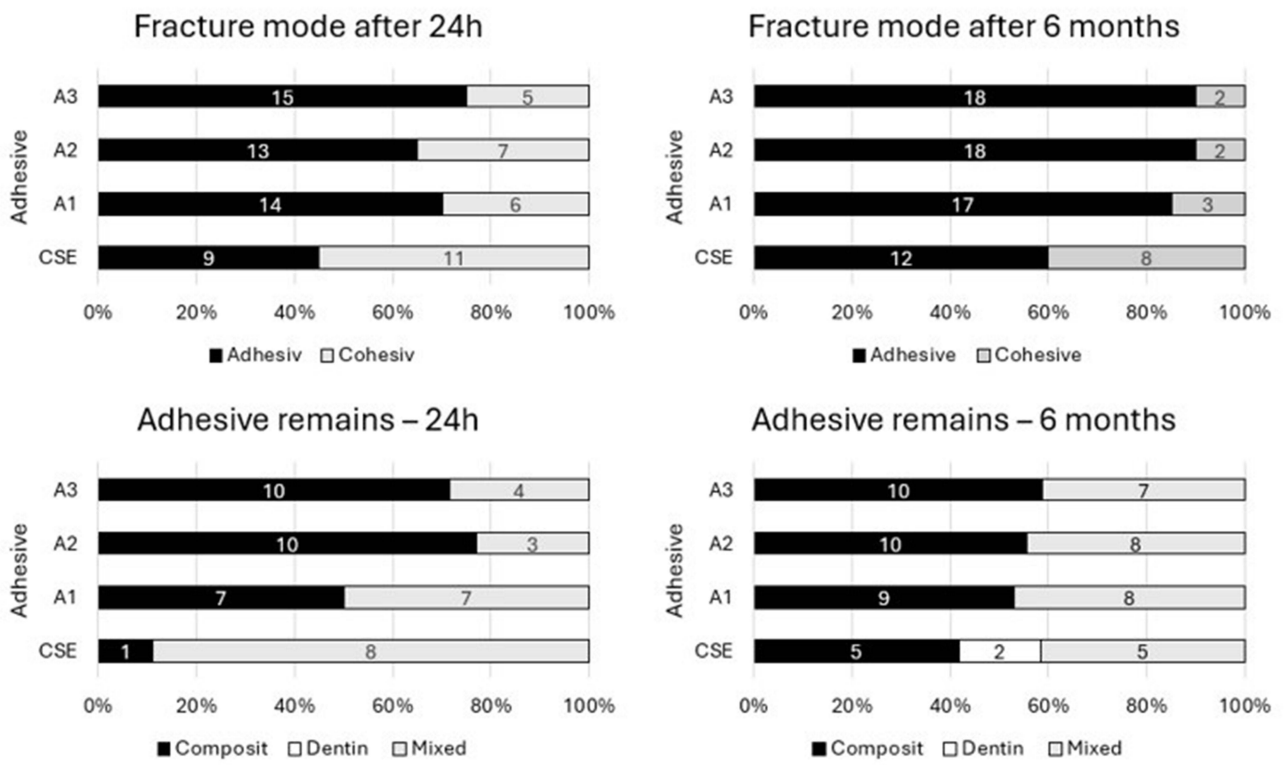

Figure 4 Fracture modes after 24h and 6 months and distribution of localization of the adhesive remains after 24h and 6 months.

SEM Analysis

Representatively, Figure 5 presents SEM images taken at 6 months, showing the dentin-composite interface for adhesives A1 and A3. Both adhesives display resin tag formation, though A3 appears to form a thicker adhesive layer. Figure 6 shows distinct capsular structures featuring a central core presumably embedded into a hydroxyapatite nanocrystal. An evenly distribution of the nanocapsules throughout the matrix with no signs of aggregation can be observed, suggesting a successful dispersion.

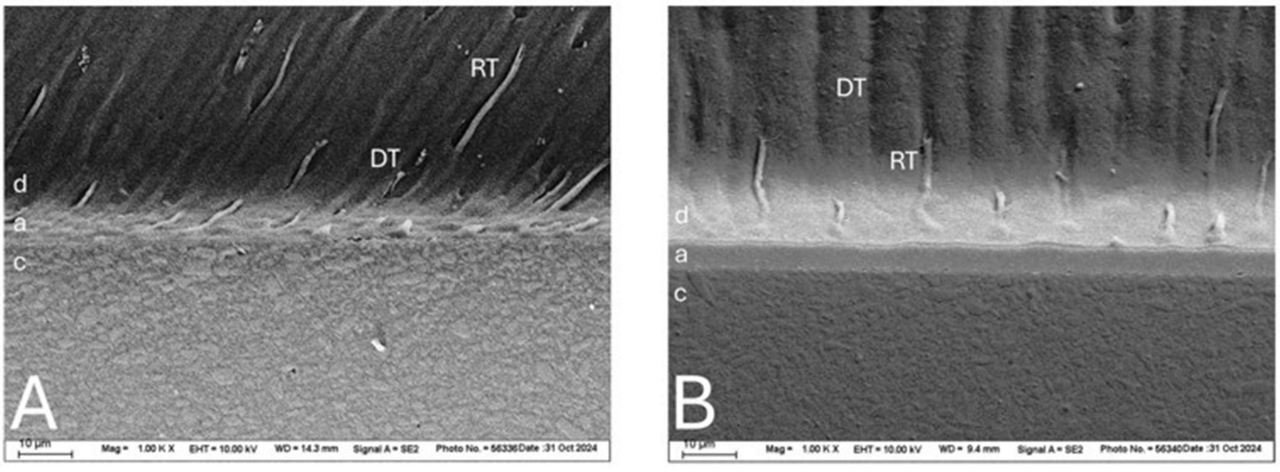

Figure 5 Scanning electron microscope (SEM) pictures of the groups A1 (**A**) and A3 (**B**).
Abbreviations: d, dentin; a, adhesive layer; c, composite; DT, dentin tubulus; RT, resin tag.

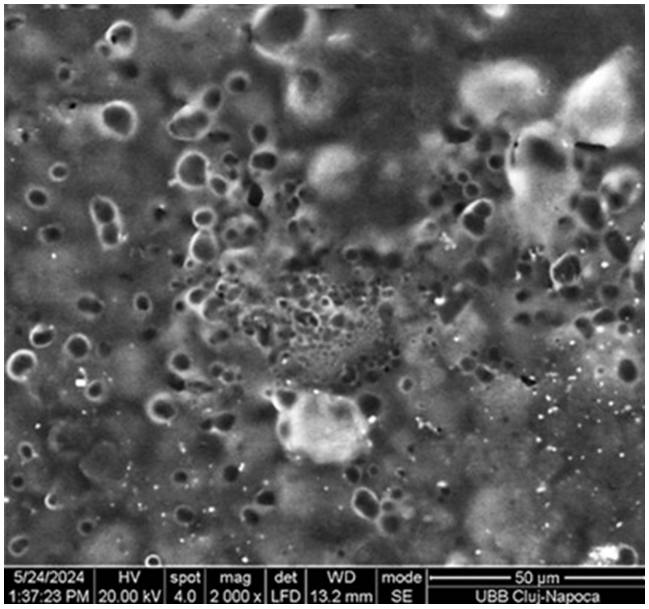

Figure 6 Scanning electron microscope (SEM) picture of the produced nanocapsules.

Nano-IR sSNOM Imaging

Figure 7 shows a representative nano-IR image of a 30×30 µm^2 area (400 x 400 pixels) capturing the resin composite (C) on the left side of the image bounded by the experimental adhesive (A) to the dentin structure (D). A dentin tubule (DT) thoroughly infiltrated with adhesive is also visible in the dentin area. The left image represents the topography of the measured area, followed by nano-IR absorption and reflectivity images, both at a wavelength of 1030 cm^{-1}. The selected wavelength enables a clear distinction between the inorganic components - the silicate glass filler in the composite and the hydroxyapatite in the tooth area - in contrast to the organic components - methacrylate polymer and collagen. The absorption image identified the methacrylate in the organic matrix of the composite and the experimental adhesive, as well as the collagen in the dentin structure, as areas of low absorption (blue). In addition, it also allows the delineation of the hybrid layer (HL), ie, the interaction of the adhesive with the dentin structure, as an area of intermediate absorption between the adhesive and the tooth structure. The image also demonstrates that the dentinal tubule (DT) was completely filled with the adhesive, showing good infiltration of the experimental adhesive and the development of dentin tags able to strengthen the bond. The silicate glass

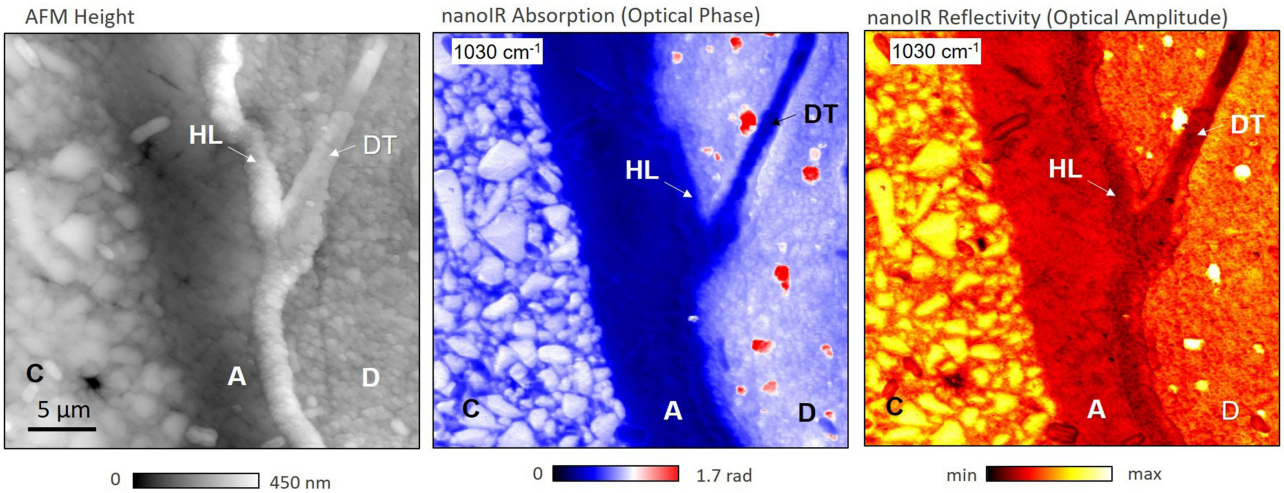

Figure 7 nanoIR chemical mapping of the tooth sample: topography, absorption, and reflectivity at 1030 cm^{-1}.
Abbreviations: A, adhesive; C, composite; D, dentin; DT, dentin tubule; HL, hybrid layer.

https://doi.org/10.2147/IJN.S525646

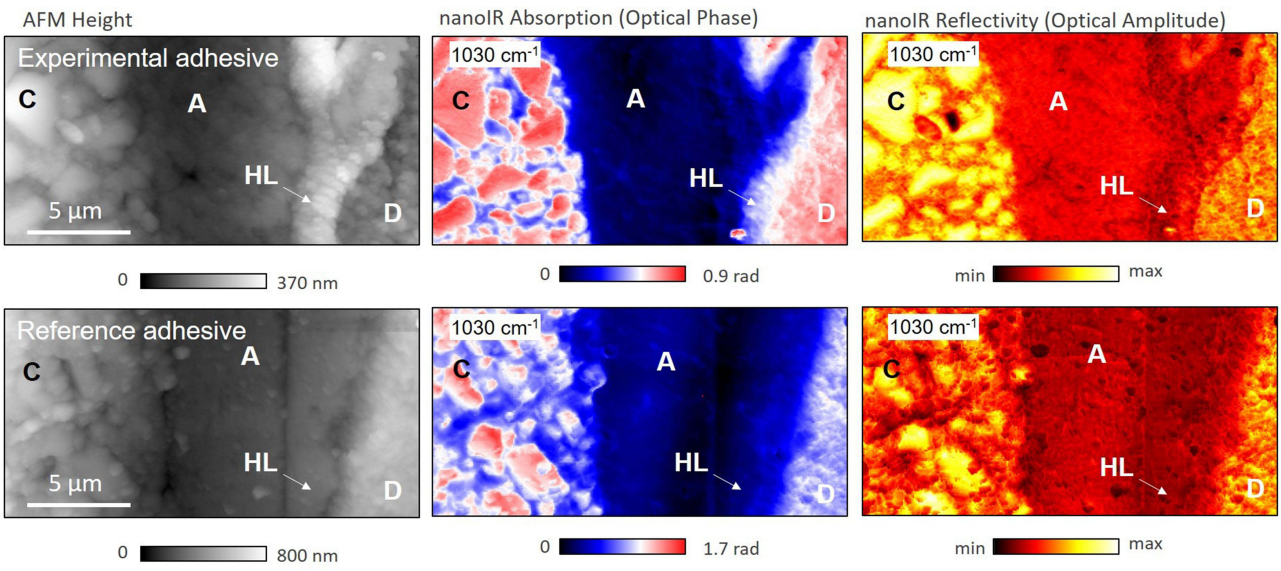

Figure 8 Representative nanoIR images for comparison between the reference adhesive CSE and the experimental adhesive A2.
Abbreviations: A, adhesive; C, composite; D, dentin; DT, dentin tubule; HL, hybrid layer.

fillers contained in the composite material are clearly distinguishable and are characterized by high absorption (grey-white) at 1030 cm^{-1}, similar to hydroxyapatite (white) in dentin. The dentin area shows spots (strong absorption, red) due to hypermineralization or precipitates that formed on the dentin surface. The described structures are conform with the AFM and reflectivity images.

Following the same methodology, Figure 8 shows representative nano-IR images of 20×10 μm^2 areas (300 x 150 pixels), measured comparatively in the reference adhesive CSE and the experimental adhesive A2. The adhesive A2 contains a lower concentration of nanocapsules as A3 and therefore serves as a "worst-case" scenario, since A3 is supposed to perform similar or slightly better. The characteristic features described above are clearly visible here, which indicates a good interaction of both adhesives with the tooth structure and a well-developed hybrid layer as an interaction product.

Discussion

The phenolic compounds in green tea primarily consist of catechin derivatives, although smaller amounts of other compounds, such as flavonols and phenolic acids, are also present. Flavonoids, a key group of phenolic compounds, are classified into several subclasses: flavonols, anthocyanidins, flavones, isoflavones, flavanones, and flavanols. In addition to flavonoids, phenolic acids represent another significant group, categorized into hydroxycinnamic and hydroxybenzoic acids. Gallic acid, a relatively simple compound synonymously called 3,4,5-trihydroxybenzoic acid, serves as the foundational structure for hydroxybenzoic acids and their derivatives, such as ellagic acid, which exhibit antioxidant properties. Similarly, hydroxycinnamic acid derivatives are based on p-coumaric acid, characterized by an aromatic ring with a hydroxy substitution and a propenoic acid group.[54] One of the catechins, mainly found in the buds and first leaves of green tea, is epigallocatechin gallate (EGCG), a flavonoid with excellent biocompatibility and low toxicity,[55] as well as anti-inflammatory, antioxidant, antifibrotic, anti-remodeling, and tissue-protective properties.[56] Using data from studies on the interactions of compounds found in GTE, other polyphenols such as epicatechin-3-gallate, gallocatechin, and epicatechin[57] have been demonstrated to be less effective in inhibiting MMPs. However, they have been shown to exert a synergistic effect in conjunction with EGCG.[58] Considering these synergistic effects, the current study employed not only EGCG but an extract comprising all the previously mentioned polyphenols, aiming to maximize the effect on improving or alleviating the impact of aging on bond strength.[58] It is hypothesized that the flavonoids present in green tea can enhance the mechanical characteristics of collagen by enabling crosslinking even in an acidic milieu. Furthermore, these compounds are highly reactive with proteins and can scavenge free radicals.[41,59,60] EGCG has been demonstrated to exert a considerable inhibitory effect on MMPs, thereby helping to preserve the integrity of the dentin matrix and

maintain bonding strength.[32,61] The most significant value of inhibition is thereby observed in the counteraction of the activity of MMP-2 and -9.[62,63] Although the precise inhibition process remains uncertain, an increasing body of evidence suggests that this effect is likely achieved by stopping the activation of MMPs by suppressing the production of their antecedents and activator proteins.[64] Another beneficial effect shown by EGCG is the retainment of the bonding durability through forming a bond with the resin present on the hybrid layer, thereby inhibiting the effects of MMPs in an additional way.[65] As far as the understanding of MMP deactivation remains limited, the process of MMP activation is therefore better understood. A great variety of research proved the activating effect of acidity on the MMPs. The activation of latent purified forms of human MMP-2, MMP-8, and MMP-9 has been confirmed in environments with a pH of 4.5 or lower.[30] As mild self-etch adhesives possess a pH of approximately two while bonding,[36] thereby activating MMPs, the objective of the present study was to counteract the self-limiting factors of adhesives by adding green tea extract (GTE). In addition to targeting the MMP deactivating effect, the idea of using EGCG was also based on the hypothesis that collagen itself is affected by polyphenols. Thus, EGCG plays an essential role in stabilizing the triple-helical structure of collagen and, consequently, its resistance to collagenase,[66] enhancement of the mechanical properties, and resistance to enzymatic degradation of the collagen matrix through intra- and intermolecular crosslinking.[67] Incorporating GTE-filled nanocapsules into adhesives is a modern approach, utilizing the characteristics of established MMP inhibitors and combining them with the new possibilities of distribution and release brought by nanotechnology.[16]

In fact, HPLC proved that the implementation of GTE into the nanocapsules was successful. Additionally, spectrophotometer analysis confirmed the release of polyphenols from both the capsule and the adhesive containing the capsules. In addition, the experimental adhesives produced, although not yet optimized and in an early development phase, were comparable in their bonding ability to the commercially available gold standard unanimously accepted today. The quantitative determination of polyphenols using both HPLC and spectrophotometric methods enables the precise optimization of experimental adhesives. These findings confirm their ability to create a strong bond and form a uniform hybrid layer.

Applying the principle of collagen crosslinking described above to the present study should result in higher SBS due to forming a stronger bond to the exposed human dentin. However, this effect was not seen as a direct improvement in SBS values but somewhat indirectly through the stability of bond over time, as observed in the Weibull analysis – where the values for the experimental adhesives remained respectively stable over time, while those for CSE showed a decrease. As the experimental adhesives were not explicitly optimized for compatibility with the primer, this might explain the lack of improvement in SBS values compared to CSE.

10-Methacryloyloxydecyl dihydrogen phosphate (MDP) monomers are known for their strong chemical affinity to hydroxyapatite (HAP), the mineral component of dentin and enamel. MDP forms a stable calcium-phosphate complex with HAP through ionic interactions, creating a durable bond that resists hydrolytic degradation. This bond helps to improve adhesive longevity and contributes to a more stable hybrid layer over time by reducing the likelihood of breakdown in moist environments.[68] MDP monomers are present in the primer used for all adhesives and CSE. Although the experimental adhesives lack MDP monomers, they demonstrate sufficient stability even after a 6-month aging period. The findings of this study indicate that while MDP enhances bond durability through its strong affinity for hydroxyapatite, the structural integrity of the experimental adhesives remains acceptable over time. This can be attributed to the polyphenols' crosslinking interactions with the collagen matrix.

The Weibull modulus has been demonstrated to be a fundamental parameter in comparing the reliability of mechanical properties in brittle materials. Therefore, a higher modulus points to a greater reliability and reduced variability in the material's performance, whereas a lower modulus reflects increased variation in bond strength results, indicating reduced predictability over time.[69] Considering only the experimental adhesives, the GTE-capsule-infused adhesives initially show weaker performance compared to their unfilled counterpart A1 after 24 hours; however, after a six-month interval, their performance becomes comparable. When also taking CSE into account, it stands out with significantly higher reliability than all experimental adhesives but undergoes a significant decrease due to aging. The only experimental adhesive showing a small but significant decrease in reliability is A3, which may point to an upper limit for incorporated nanocapsules, which, when exceeded, might weaken the bond strength and reliability, resulting in greater scatter and inconsistency. The slightly lower SBS values may be attributed to the used primer not being fully

synchronized to the experimental adhesives and the capsules' composition. As the capsule shell is formed from polymers, they might not be fully incorporated into the polymer matrix, creating potential fracture points. As the release of GTE would still occur, its crosslinking characteristics are a possible explanation for the higher reliability. Further, all groups were unaffected by aging.

A different explanation for the slightly higher SBS values of CSE can be found with the help of fractographic analysis, as the inclusion of cohesive failures into statistics results in a distortion of data. By analyzing the data, it is conductible that a higher SBS seems to be associated with a cohesive failure. This effect can be explained as an exact SBS can only be calculated given an adhesive failure modulus. Cohesive failures in dentin or composite make it impossible to accurately calculate the bonded surface area for SBS measurements, as the surface is uneven and, therefore, much larger.[70] Consequently, the calculated SBS values will be incorrectly larger because the force was divided by a significantly smaller area than the fractography indicates. Moreover, the data indicates that while cohesive failure initially represents the dominant failure mode (55%) in CSE, its occurrence declines to 40% after aging, indicating a reduction in cohesive failures over time. Considering only adhesive failures, slight differences observed at 24h immersion, as those between CSE and A3, are no longer evident after aging, making the experimental adhesives equal to the gold standard adhesive CSE. As previously discussed, EGCG proved to strengthen the collagen helicase; the argument may explain the reduced amount of cohesive failures, particularly after a six-month aging period in the GTE-capsule-infused adhesives. Additionally, excluding cohesive failures also revealed no statistically significant impact of aging.

Incorporating unencapsulated GTE into an experimental adhesive comparable to a reference without GTE effectively improved SBS and Weibull-modulus in a comparable study design. However, the amount used was 9.38% by weight, significantly higher than the 3.05% by weight of GTE used in the nanocapsules in the present research. This provides a clear indication that the GTE amount used should be increased accordingly for further optimization.[45] The smaller amount of GTE used may be a reasonable explanation for the results mentioned above, as there may need to be more GTE present in the system to realize the potential of its dentin-strengthening effects via crosslinking fully. It can be surmised that a greater initial quantity of GTE should be present within the system to capitalize fully on its beneficial properties. Consequently, it may be feasible to incorporate not only capsules but also unencapsulated GTE into the adhesive.

Conclusion

The integration of GTE into nanocapsules was successful and proven to be a promising concept for synthesizing modern adhesives. Although the amount of GTE introduced was insufficient as it failed to improve the bond strength to the tooth structure, the experimental adhesives demonstrated consistent reliability during aging compared to the gold standard adhesive, which experienced a decline in this regard. Moreover, the innovative analytical tool used to nano-IR imaging the interaction between adhesive and tooth substance proved to be helpful in closing a nano-analytical diagnostic gap in the molecular spectroscopy of dental nanomaterials.

Data Sharing Statement

Data will be made available on request.

Acknowledgments

The authors are grateful to VOCO GmbH for providing the polymer-based composite material used in the study.

Author Contributions

All authors made a significant contribution to the work reported, whether that is in the conception, study design, execution, acquisition of data, analysis and interpretation, or in all these areas; took part in drafting, revising or critically reviewing the article; gave final approval of the version to be published; have agreed on the journal to which the article has been submitted; and agree to be accountable for all aspects of the work.

Funding

This research received no specific grant from funding agencies in the public, commercial, or not-for-profit sectors.

Disclosure

The authors declare that they have no known competing financial interests or personal relationships that could have appeared to influence the work reported in this paper.

References

1. Vert M, Doi Y, Hellwich K-H, et al. Terminology for biorelated polymers and applications (IUPAC Recommendations 2012). *Pure Appl Chem*. 2012;84(2):377–410. doi:10.1351/PAC-REC-10-12-04
2. Pati R, Shevtsov M, Sonawane A. Nanoparticle vaccines against infectious diseases. *Front Immunol*. 2018;9:2224. doi:10.3389/fimmu.2018.02224
3. Granata G, Stracquadanio S, Leonardi M, et al. Essential oils encapsulated in polymer-based nanocapsules as potential candidates for application in food preservation. *Food Chem*. 2018;269:286–292. doi:10.1016/j.foodchem.2018.06.140
4. Yan B, Davachi SM, Ravanfar R, et al. Improvement of vitamin C stability in vitamin gummies by encapsulation in casein gel. *Food Hydrocoll*. 2021;113:106414. doi:10.1016/j.foodhyd.2020.106414
5. Thakur VK, Kessler MR. Self-healing polymer nanocomposite materials: a review. *Polymer*. 2015;69:369–383. doi:10.1016/j.polymer.2015.04.086
6. Kipp JE. The role of solid nanoparticle technology in the parenteral delivery of poorly water-soluble drugs. *Int J Pharm*. 2004;284(1–2):109–122. doi:10.1016/j.ijpharm.2004.07.019
7. Prasanna P, Kumar P, Kumar S, et al. Current status of nanoscale drug delivery and the future of nano-vaccine development for leishmaniasis - A review. *Biomed Pharmacother*. 2021;141:111920. doi:10.1016/j.biopha.2021.111920
8. Bertrand N, Leroux JC. The journey of a drug-carrier in the body: an anatomo-physiological perspective. *J Control Release*. 2012;161(2):152–163. doi:10.1016/j.jconrel.2011.09.098
9. O'Brien MER, Wigler N, Inbar M, et al. Reduced cardiotoxicity and comparable efficacy in a Phase III trial of pegylated liposomal doxorubicin HCl (CAELYX/Doxil) versus conventional doxorubicin for first-line treatment of metastatic breast cancer. *Ann Oncol*. 2004;15(3):440–449. doi:10.1093/annonc/mdh097
10. Keleş S, Alakbarli J, Akgül B, et al. Nanotechnology based drug delivery systems for malaria. *Int J Pharm*. 2024;666:124746. doi:10.1016/j.ijpharm.2024.124746
11. Feynman R. There's plenty of room at the bottom. *Resonance*. 2011;16(9):1.
12. Hitchcock J, White AL, Hondow N, et al. Metal-shell nanocapsules for the delivery of cancer drugs. *J Colloid Interface Sci*. 2020;567:171–180. doi:10.1016/j.jcis.2019.12.018
13. Pendleton JN, Gilmore BF. The antimicrobial potential of ionic liquids: a source of chemical diversity for infection and biofilm control. *Int J Antimicrob Agents*. 2015;46(2):131–139. doi:10.1016/j.ijantimicag.2015.02.016
14. Ferraz R, Branco LC, Prudêncio C, Noronha JP, Petrovski Z. Ionic liquids as active pharmaceutical ingredients. *ChemMedChem*. 2011;6(6):975–985. doi:10.1002/cmdc.201100082
15. Cuppini M, Garcia IM, Souza VSD, et al. Ionic liquid-loaded microcapsules doped into dental resin infiltrants. *Bioact Mater*. 2021;6(9):2667–2675. doi:10.1016/j.bioactmat.2021.02.002
16. Siepmann J, Siepmann F. Mathematical modeling of drug delivery. *Int J Pharm*. 2008;364(2):328–343. doi:10.1016/j.ijpharm.2008.09.004
17. Gendron R, Grenier D, Sorsa T, Mayrand D. Inhibition of the activities of matrix metalloproteinases 2, 8, and 9 by chlorhexidine. *Clin Diagn Lab Immunol*. 1999;6(3):437–439. doi:10.1128/CDLI.6.3.437-439.1999
18. Priyadarshini BM, Selvan ST, Lu TB, Xie H, Neo J, Fawzy AS. Chlorhexidine nanocapsule drug delivery approach to the resin-dentin interface. *J Dent Res*. 2016;95(9):1065–1072. doi:10.1177/0022034516656135
19. Frassetto A, Breschi L, Turco G, et al. Mechanisms of degradation of the hybrid layer in adhesive dentistry and therapeutic agents to improve bond durability—A literature review. *Dent Mater*. 2016;32(2):e41–e53. doi:10.1016/j.dental.2015.11.007
20. Zhang S, Kern M. The role of host-derived dentinal matrix metalloproteinases in reducing dentin bonding of resin adhesives. *Int J Oral Sci*. 2009;1(4):163–176. doi:10.4248/IJOS.09044
21. Linde A, Goldberg M. Dentinogenesis. *Crit Rev Oral Biol Med*. 1993;4(5):679–728. doi:10.1177/10454411930040050301
22. Mazzoni A, Mannello F, Tay FR, et al. Zymographic analysis and characterization of MMP-2 and -9 forms in human sound dentin. *J Dent Res*. 2007;86(5):436–440. doi:10.1177/154405910708600509
23. Mazzoni A, Papa V, Nato F, et al. Immunohistochemical and biochemical assay of MMP-3 in human dentine. *J Dent*. 2011;39(3):231–237. doi:10.1016/j.jdent.2011.01.001
24. Sulkala M, Larmas M, Sorsa T, Salo T, Tjäderhane L. The localization of matrix metalloproteinase-20 (MMP-20, Enamelysin) in mature human teeth. *J Dent Res*. 2002;81(9):603–607. doi:10.1177/154405910208100905
25. Tersariol IL, Geraldeli S, Minciotti CL, et al. Cysteine cathepsins in human dentin-pulp complex. *J Endod*. 2010;36(3):475–481. doi:10.1016/j.joen.2009.12.034
26. Sulkala M, Tervahartiala T, Sorsa T, Larmas M, Salo T, Tjäderhane L. Matrix metalloproteinase-8 (MMP-8) is the major collagenase in human dentin. *Arch Oral Biol*. 2007;52(2):121–127. doi:10.1016/j.archoralbio.2006.08.009
27. Van Strijp AJP, Jansen DC, DeGroot J, Ten Cate JM, Everts V. Host-derived proteinases and degradation of dentine collagen in situ. *Caries Res*. 2003;37(1):58–65. doi:10.1159/000068223
28. Tjäderhane L, Salo T, Larjava H, Larmas M, Overall CM. A novel organ culture method to study the function of human odontoblasts in vitro: gelatinase expression by odontoblasts is differentially regulated by TGF-β1. *J Dent Res*. 1998;77(7):1486–1496. doi:10.1177/00220345980770070301
29. Martin-De Las Heras S, Valenzuela A, Overall CM. The matrix metalloproteinase gelatinase A in human dentine. *Arch Oral Biol*. 2000;45(9):757–765. doi:10.1016/S0003-9969(00)00052-2
30. Tjäderhane L, Larjava H, Sorsa T, Uitto V-J, Larmas M, Salo T. The activation and function of host matrix metalloproteinases in dentin matrix breakdown in caries lesions. *J Dent Res*. 1998;77(8):1622–1629. doi:10.1177/00220345980770081001
31. Pashley DH, Tay FR, Yiu C, et al. Collagen degradation by host-derived enzymes during aging. *J Dent Res*. 2004;83(3):216–221. doi:10.1177/154405910408300306

32. Hashimoto M, Ohno H, Kaga M, Endo K, Sano H, Oguchi H. In vivo degradation of resin-dentin bonds in humans over 1 to 3 years. *J Dent Res*. 2000;79(6):1385–1391. doi:10.1177/00220345000790060601
33. Davis GE. Identification of an abundant latent 94-kDa gelatin-degrading metalloprotease in human saliva which is activated by acid exposure: implications for a role in digestion of collagenous proteins. *Arch Biochem Biophys*. 1991;286(2):551–554. doi:10.1016/0003-9861(91)90078-W
34. Nishitani Y, Yoshiyama M, Wadgaonkar B, et al. Activation of gelatinolytic/collagenolytic activity in dentin by self-etching adhesives. *Eur J Oral Sci*. 2006;114(2):160–166. doi:10.1111/j.1600-0722.2006.00342.x
35. Hass V, Luque-Martinez IV, Gutierrez MF, et al. Collagen cross-linkers on dentin bonding: stability of the adhesive interfaces, degree of conversion of the adhesive, cytotoxicity and in situ MMP inhibition. *Dent Mater*. 2016;32(6):732–741. doi:10.1016/j.dental.2016.03.008
36. Van Meerbeek B, Yoshihara K, Yoshida Y, Mine A, De Munck J, Van Landuyt KL. State of the art of self-etch adhesives. *Dent Mater*. 2011;27(1):17–28. doi:10.1016/j.dental.2010.10.023
37. Graham HN. Green tea composition, consumption, and polyphenol chemistry. *Prev Med*. 1992;21(3):334–350. doi:10.1016/0091-7435(92)90041-f
38. Khan N, Mukhtar H. Tea and health: studies in humans. *Curr Pharm Des*. 2013;19(34):6141–6147. doi:10.2174/1381612811319340008
39. Haslam E. Natural polyphenols (Vegetable Tannins) as drugs: possible modes of action. *J Nat Prod*. 1996;59(2):205–215. doi:10.1021/np960040
40. Xu X, Zhou XD, Wu CD. The tea catechin epigallocatechin gallate suppresses cariogenic virulence factors of Streptococcus mutans. *Antimicrob Agents Chemother*. 2011;55(3):1229–1236. doi:10.1128/AAC.01016-10
41. Lim E, Lim M-J, Min K-S, et al. Effects of epicatechin, a crosslinking agent, on human dental pulp cells cultured in collagen scaffolds. *J Appl Oral Sci*. 2016;24(1):76–84. doi:10.1590/1678-775720150383
42. Yuan X, Wang Q, Zhao Q, Bai Z, Chen C, Xie H. Inhibition of matrix metalloproteinase-9 by 10-MDP and its calcium salt contributes to improved dentin-bonding durability. *Int J Adhes Adhes*. 2023;120:103302. doi:10.1016/j.ijadhadh.2022.103302
43. Yu J, Zhao Y, Shen Y, et al. Enhancing adhesive–dentin interface stability of primary teeth: from ethanol wet-bonding to plant-derived polyphenol application. *J Dent*. 2022;126:104285. doi:10.1016/j.jdent.2022.104285
44. Lewis NV, Aggarwal S, Borse NN, et al. The effect of matrix metalloproteinase inhibitors on the microtensile bond strength of dentin bonding agents in caries affected dentin: a systematic review. *J Int Soc Prev Community Dent*. 2023;13(3):173–184. doi:10.4103/jispcd.JISPCD_5_23
45. Schröter F-J, Moldovan M, Sarosi C, Ilie N. Enhancing dentin bonding through new adhesives formulations with natural polyphenols, tricalcium phosphate and chitosan. *Dent Mater*. 2024;40(2):276–284. doi:10.1016/j.dental.2023.11.014
46. Beck F, Ilie N. Antioxidants and collagen-crosslinking: benefit on bond strength and clinical applicability. *Materials*. 2020;13(23). doi:10.3390/ma13235483
47. Islam S, Hiraishi N, Nassar M, Yiu C, Otsuki M, Tagami J. Effect of natural cross-linkers incorporation in a self-etching primer on dentine bond strength. *J Dent*. 2012;40(12):1052–1059. doi:10.1016/j.jdent.2012.08.015
48. Smith BC. *Infrared Spectral Interpretation: A Systematic Approach*. 1st ed. CRC Press; 1999. doi:10.1201/9780203750841
49. Filip M, Silaghi-Dumitrescu L, Prodan D, Sarosi C, Moldovan M, Cojocaru I. Analytical approaches for characterization of teeth whitening gels based on natural extracts. *KEM*. 2017;752:24–28. doi:10.4028/www.scientific.net/KEM.752.24
50. Folin O, Ciocalteu V. On tyrosine and tryptophane determinations in proteins. *J Biol Chem*. 1927;73(2):627–650. doi:10.1016/S0021-9258(18)84277-6
51. Singleton VL, Orthofer R, Lamuela-Raventós RM. Analysis of total phenols and other oxidation substrates and antioxidants by means of Folin-Ciocalteu reagent. *Methods Enzymol*. 1999;299:152–178.
52. International Organization for Standardization Geneva, Switzerland, 2013. *Standards I. ISO 29022 Dentistry–Adhesion–Notched-Edge Shear Bond Standards I. ISO 29022 Dentistry–Adhesion–Notched-Edge Shear Bond Strength Test*.
53. Dinneen LC, Blakesley BC. Algorithm AS 62: a generator for the sampling distribution of the Mann-Whitney U Statistic. *Appl Stat*. 1973;22(2):269. doi:10.2307/2346934
54. Lorenzo JM, Munekata PES. Phenolic compounds of green tea: health benefits and technological application in food. *Asian Pac J Trop Biomed*. 2016;6(8):709–719. doi:10.1016/j.apjtb.2016.06.010
55. Hsu YW, Tsai CF, Chen WK, Huang CF, Yen CC. A subacute toxicity evaluation of green tea (Camellia sinensis) extract in mice. *Food Chem Toxicol*. 2011;49(10):2624–2630. doi:10.1016/j.fct.2011.07.007
56. Mokra D, Joskova M, Mokry J. Therapeutic effects of green tea polyphenol (–)-Epigallocatechin-3-Gallate (EGCG) in relation to molecular pathways controlling inflammation, oxidative stress, and apoptosis. *Int J Mol Sci*. 2022;24(1):340. doi:10.3390/ijms24010340
57. Ashihara H, Deng WW, Mullen W, Crozier A. Distribution and biosynthesis of flavan-3-ols in Camellia sinensis seedlings and expression of genes encoding biosynthetic enzymes. *Phytochemistry*. 2010;71(5):559–566. doi:10.1016/j.phytochem.2010.01.010
58. Suganuma M, Okabe S, Kai Y, Sueoka N, Sueoka E, Fujiki H. Synergistic effects of (−)-epigallocatechin gallate with (−)-epicatechin, sulindac, or tamoxifen on cancer-preventive activity in the human lung cancercell line PC-91. *Cancer Res*. 1999;59(1):44–47.
59. Petti S, Scully C. Polyphenols, oral health and disease: a review. *J Dent*. 2009;37(6):413–423. doi:10.1016/j.jdent.2009.02.003
60. Hiraishi N, Sono R, Sofiqul I, et al. In vitro evaluation of plant-derived agents to preserve dentin collagen. *Dent Mater*. 2013;29(10):1048–1054. doi:10.1016/j.dental.2013.07.015
61. Demeule M, Brossard M, Pagé M, Gingras D, Béliveau R. Matrix metalloproteinase inhibition by green tea catechins. *Biochim Biophys Acta*. 2000;1478(1):51–60. doi:10.1016/s0167-4838(00)00009-1
62. Koh YW, Choi EC, Kang SU, et al. Green tea (−)-epigallocatechin-3-gallate inhibits HGF-induced progression in oral cavity cancer through suppression of HGF/c-Met. *J Nutr Biochem*. 2011;22(11):1074–1083. doi:10.1016/j.jnutbio.2010.09.005
63. Yun J-H, Pang E-K, Kim C-S, et al. Inhibitory effects of green tea polyphenol (-)-epigallocatechin gallate on the expression of matrix metalloproteinase-9 and on the formation of osteoclasts. *J Periodontal Res*. 2004;39(5):300–307. doi:10.1111/j.1600-0765.2004.00743.x
64. Annabi B, Lachambre MP, Bousquet-Gagnon N, Page M, Gingras D, Beliveau R. Green tea polyphenol (-)-epigallocatechin 3-gallate inhibits MMP-2 secretion and MT1-MMP-driven migration in glioblastoma cells. *Biochim Biophys Acta*. 2002;1542(1–3):209–220. doi:10.1016/S0167-4889(01)00187-2
65. Du X, Huang X, Huang C, Wang Y, Zhang Y. Epigallocatechin-3-gallate (EGCG) enhances the therapeutic activity of a dental adhesive. *J Dent*. 2012;40(6):485–492. doi:10.1016/j.jdent.2012.02.013
66. Goo HC, Hwang YS, Choi YR, Cho HN, Suh H. Development of collagenase-resistant collagen and its interaction with adult human dermal fibroblasts. *Biomaterials*. 2003;24(28):5099–5113. doi:10.1016/S0142-9612(03)00431-9

67. Garcia-Contreras R, Chavez-Granados PA, Jurado CA, Aranda-Herrera B, Afrashtehfar KI, Nurrohman H. Natural bioactive epigallocatechin-gallate promote bond strength and differentiation of odontoblast-like cells. *Biomimetics*. 2023;8(1):75. doi:10.3390/biomimetics8010075
68. Inoue S, Koshiro K, Yoshida Y, et al. Hydrolytic stability of self-etch adhesives bonded to dentin. *J Dent Res*. 2005;84(12):1160–1164. doi:10.1177/154405910508401213
69. Quinn JB, Quinn GD. A practical and systematic review of Weibull statistics for reporting strengths of dental materials. *Dent Mater*. 2010;26(2):135–147. doi:10.1016/j.dental.2009.09.006
70. Versluis A, Tantbirojn D, Douglas WH. Why do shear bond tests pull out dentin? *J Dent Res*. 1997;76(6):1298–1307. doi:10.1177/00220345970760061001